PHENOTYPIC CHARACTER EXTRACTION OF TOMATO PLANT BASED ON 3D POINT CLOUD DATA
/
基于三维点云的番茄植株表型特征提取

Yang RAN[1)], Shilong GE[2)], Mingyuan YAO[3)], Yuxi LI[2)], Ruicheng QIU[1)], Chen WANG[3)], Li LI*[1)]

[1)] Key Laboratory of Agricultural Information Acquisition Technology, Ministry of Agriculture and Rural Affairs, China Agricultural University, Beijing / China;

[2)] Key Laboratory of Smart Agriculture System Integration, Ministry of Education, China Agricultural University, Beijing / China;

[3)] College of Information and Electrical Engineering, China Agricultural University, Beijing / China;

Corresponding author: Li Li E-mail: Lily@cau.edu.cn

DOI: https://doi.org/10.35633/inmateh-78-50

Keywords: *Phenotypic Character, 3D Reconstruction, SAC-IA, ICP, Tomato*

ABSTRACT

To address the issue of 3D reconstruction information loss caused by occlusion during single-view camera acquisition of crop phenotypic parameters, this study proposes a detection method for tomato plant phenotypic parameters based on multi-view 3D point cloud reconstruction. The Kinect 2.0 sensor was employed to acquire point cloud data of tomato plants from three different viewpoints. Background noise was effectively removed using a combination of Conditional Filtering and Statistical Outlier Removal methods. By extracting surface normal features and calculating Fast Point Feature Histograms (FPFH), the Sample Consensus Initial Alignment (SAC-IA) and Iterative Closest Point (ICP) algorithms were utilized to accomplish coarse and accurate registration of the point clouds, respectively, ultimately achieving 3D reconstruction. Experimental results demonstrated that the reconstructed 3D model of the tomato plant was clear in outline and complete in structure. For the phenotypic parameters of plant height, canopy width, and leaf angle, the coefficients of determination (R^2) between the calculated and manually measured values were 0.98, 0.94, and 0.89, respectively, with Root Mean Square Errors (RMSE) of 0.75 cm, 1.10 cm, and 4.43 °. Compared to single-view measurements, the accuracy of plant height and maximum canopy width derived from multi-view reconstruction increased by 15.31% and 13.12%, respectively. This method provides technical support for the rapid and accurate extraction of phenotypic parameters in tomato plants.

摘要

针对摄像头单视角采集作物表型参数过程中因遮挡导致三维重建信息缺失的问题，提出一种基于多视角三维点云重建的番茄植株表型参数检测方法。采用 Kinect 2.0 传感器获取三个不同视角番茄植株的点云数据，利用条件滤波与统计离群点移除方法去除背景噪声。通过提取表面法线特征并计算快速点特征直方图（FPFH），利用采样一致性初始配准（SAC-IA）与迭代最近点（ICP）算法完成点云的粗配准与精配准，实现三维重建。实验结果表明，重建后的番茄植株三维模型外形轮廓清晰、结构完整。植株株高、最大冠幅和叶夹角等表型参数，计算值与实测值的决定系数 R^2分别为 0.98、0.94 和 0.89，均方根误差 RMSE 分别为 0.75 cm、1.10 cm 和 4.43°。与单视角对比，多视角重建的株高和最大冠幅的精度分别提高了 15.31%和 13.12%。该方法为番茄植株表型参数的快速、精准提取，提供了技术支持。

INTRODUCTION

Tomatoes are rich in nutrients and are one of the most important solanaceous vegetables in the world. Tomato phenotypic parameters such as plant height, canopy width, and leaf angle effectively reflect the plant's growth and development status, which was of great significance for high-yield cultivation *(Schunck et al., 2025; Timprae et al., 2025*). Traditional methods involving manual measurement, destructive techniques, and low-throughput measurements could no longer meet the demands of intelligent agricultural management (*Jiang et al., 2025; Mach et al., 2025*).

[1] *Yang Ran, Ph.D. candidate; Shilong Ge, M.S. candidate; Mingyuan Yao, Ph.D. candidate; Yuxi Li, M.S. candidate; Ruicheng Qiu, Ph.D., Associate Professor; Chen Wang, Ph.D., Associate Professor; Li Li, Ph.D., Associate Professor.*

Therefore, how to rapidly and accurately obtain phenotypic parameters of the tomato plant has become a key challenge in the current stage (*Sun et al., 2023; Rossi et al., 2025*).

Computer vision has revolutionized plant phenotypic analysis and has become the primary method in the field (*Geng et al., 2023; Galba et al., 2025; Qi J et al., 2025*). In plant phenotyping, high-resolution RGB images captured fine details such as texture and color variations, allowing the observation of subtle plant features (*Zuo et al., 2023*). However, because plants inherently have complex three-dimensional structures, two-dimensional imaging is limited by occlusion and cannot fully represent spatial complexity (*Du et al., 2023; Choi et al., 2025*). Multi-view images captured by UAV combined with structure-from-motion (SfM) reconstruction can overcome these limitations, enabling high-precision phenotyping (*Zermas et al., 2019; James et al., 2025*). Nevertheless, in greenhouse environments, UAV operation is often hindered by physical obstructions and limited space, making reliable deployment difficult. LiDAR systems offer distinct advantages, including a large acquisition range and high measurement accuracy, and have been successfully employed for crop point cloud acquisition and phenotyping (*Jiang et al., 2023; Miao et al., 2023; Hadadi et al., 2025*). However, their widespread application in practical tomato production is constrained by high costs and the requirement for additional auxiliary equipment and wiring. In contrast, Kinect sensors are low-cost, portable, and easily integrated into acquisition platforms, offering a practical solution for multi-view point cloud collection and supporting high-throughput, automated phenotyping of crops (*Vázquez-Arellano et al., 2018; Sun et al., 2023; Shi et al., 2025*).

Therefore, this study developed a practical workflow using a Kinect 2.0 sensor to capture multi-view 3D point clouds. The acquired point clouds were processed through denoising and registration to generate complete and high-fidelity 3D model of individual tomato plant. From this reconstructed 3D model, phenotypic parameters such as plant height, canopy width, and leaf angle were extracted. this approach provides a low-cost, scalable, and robust solution for automated phenotyping, enabling rapid and accurate assessment of plant traits while providing a solid technical foundation for high-throughput phenotyping and precision agriculture applications.

MATERIALS AND METHODS

Experimental Materials and Data Acquisition

The experiment was conducted in the rooftop greenhouse of the College of Information and Electrical Engineering, China Agricultural University, located in a temperate monsoon climate zone. The test crop was pink crown tomato (Solanum lycopersicum), grown in pots. Fifty tomato seedlings were transplanted at the end of April 2024, and phenotypic data were collected in early May of the same year. The workflow for extracting tomato phenotypic traits was illustrated in Fig. 1 and consisted of point cloud preprocessing and 3D reconstruction. Tomato plants were scanned at 0°, 120°, and 240° using a Kinect 2.0 sensor, and the registered 3D point cloud was used to extract plant height, canopy width, and leaf angle for accuracy validation through error analysis.

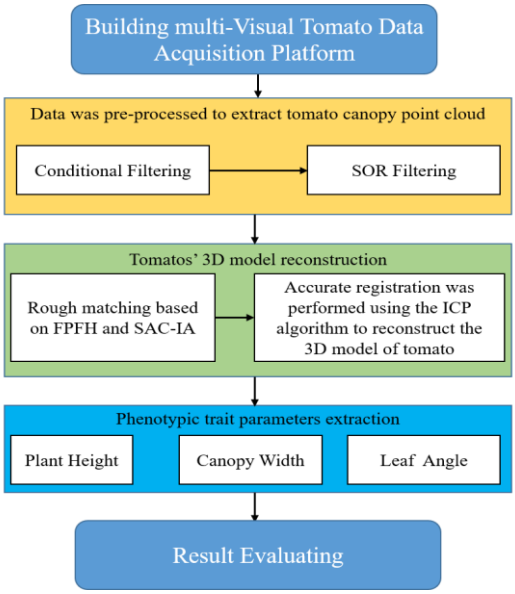

Fig. 1 - Flow chart of tomato phenotype feature extraction

Multi-view Point Cloud Data Acquisition Platform

A multi-view tomato canopy 3D data acquisition system was developed in this study. The system consisted of a Kinect 2.0 sensor, a laptop, a motorized turntable, and a tripod, with the distance between the tomato plant and the sensor was set to 70 cm, as shown in Figure 2.

Fig. 2 - Tomato plant point cloud data collection platform

Data acquisition was conducted indoors under wind-free and stable lighting conditions to minimize environmental interference. The motorized turntable was automatically controlled to rotate slowly, completing one full revolution in approximately 30 seconds. During rotation, images were captured every 10 seconds at three perspectives: 0° (Perspective 1), 120° (Perspective 2), and 240° (Perspective 3). This slow and stable rotation ensured that the tomato plants remained steady and undisturbed throughout the acquisition process.

The Kinect 2.0 sensor was connected to the laptop via USB 3.0 and operated based on Time-of-Flight (ToF) technology. It emitted modulated near-infrared light pulses and received the reflected pulses through a photosensitive module. By calculating the time difference between the emitted and received pulses, the depth of each pixel was obtained, generating a depth map that captured the spatial structure of the tomato canopy in real time. The effective depth sensing range was from 0.5 to 4.5 meters, with a measurement error of approximately 2 to 6 millimeters. This system enabled accurate and stable point cloud data acquisition of tomato plants in a short period of time. For each depth image and RGB image acquired by the Kinect 2.0 sensor, a 3D coordinate mapping relationship between color and depth information was established using the sensor's internal mapping function. After image registration, each point in the point cloud contained both 3D spatial coordinates (x, y, z) and color attributes (R, G, B). The raw point clouds collected from the three angles were shown in Figure 3.

a. Perspective 1 (0°) *b. Perspective 2 (120°)* *c. Perspective 3 (240°)*

Fig. 3 - Original point cloud of single tomato

The point cloud processing was implemented in the Ubuntu 20.04 and VSCode environment using the Point Cloud Library (PCL). The collected data were processed on an image workstation equipped with an Intel i5-9300H processor.

Point Cloud Preprocessing

When acquiring tomato point cloud data using the Kinect 2.0 sensor, a certain amount of noise and irrelevant background points was inevitable, which could affect the accuracy of spatial positioning and 3D structural reconstruction of the tomato canopy. In addition, due to the large volume of point cloud data, preprocessing was necessary to improve the reconstruction speed and accuracy.

First, condition filtering was applied to remove invalid background information. Then, the Statistical Outlier Removal (SOR) filter was used to eliminate canopy noise, thereby improving the measurement accuracy and feature recognition speed of the canopy. These preprocessing steps resulted in a clear tomato point cloud that was free from clustered outliers and better represents the canopy structure.

(1) Conditional filtering

A point cloud was a collection of points in three-dimensional space, composed of N points in D-dimensional space. When D = 3, each point can be represented by 3D Cartesian coordinates (x, y, z). Based on the common attributes of 3D point clouds, condition filtering was applied to remove irrelevant or out-of-bound points. To extract the target tomato point cloud from single-view raw data, inequality constraints were typically applied to the point coordinates, as shown in Equation (1).

$$\begin{cases} Xm < X < Xn \\ Ym < Y < Yn \\ Zm < Z < Zn \end{cases} \quad (1)$$

where: (Xm, Xn) represented the valid range of the tomato point cloud along the X-axis, which was set to [-0.15, 0.15];

(Ym, Yn) represented the valid range along the Y-axis, which was set to [-0.1, 0.3];

(Zm, Zn) represented the valid range along the Z-axis, which was set to [-0.9, -0.5];

Using these inequality constraints, the point clouds from the three different views were individually filtered. The results after filtering were shown in Figure 4.

a. Perspective 1 (0°) *b. Perspective 2 (120°)* *c. Perspective 3 (240°)*

Fig. 4 - Tomato plant point cloud processed by conditional filter

As illustrated, a significant number of noise and outlier points remain around the tomato leaves and stem. To further eliminate these outliers and noise, the Statistical Outlier Removal (SOR) algorithm was applied.

(2) SOR filtering

Raw point clouds typically contain noise, which complicated the estimation of local point cloud features such as surface normals or curvature variations and may prolong point cloud registration. The SOR filter used a statistical approach to remove outliers. Specifically, for each point, it performed statistical analysis on its k nearest neighbors and calculated the average distance to these neighbors. The algorithm assumed that the distances followed a Gaussian distribution and defined points whose average distance exceeded a predefined threshold as outliers, which were then removed from the dataset. The point cloud after SOR filtering were shown in Figure 5.

a. Perspective 1 (0°) after SOR filtering *b. Perspective 2 (120°) after SOR filtering* *c. Perspective 3 (240°) after SOR filtering*

Fig. 5 - Tomato plant point cloud processed by SOR

Multi perspective tomato 3D point cloud registration

Despite preprocessing, limitations from single-view occlusions remained. To address this, the tomato plant point clouds from three different viewpoints were registered and reconstructed. First, the point clouds obtained from the 0° and 120° views were registered and merged. Then, the result was further registered with the 240° view to obtain a complete point cloud representation of the tomato plant. Each registration process consisted of coarse and fine registration steps. The registration procedure and the results of the tomato point clouds from the three viewpoints were shown in Figure 6.

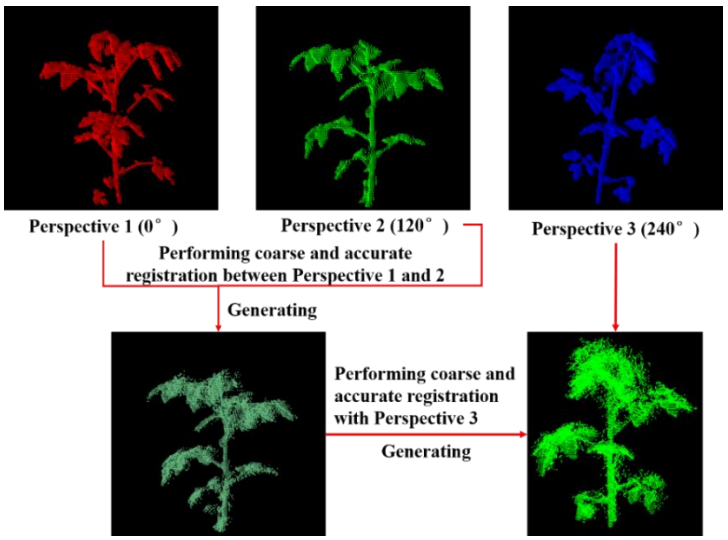

Fig. 6 - Multi perspective tomato plant point cloud reconstruction process

(1) Coarse registration

The point cloud data were first subjected to coarse registration. The process began by loading both the source and target point cloud datasets. Invalid points were then removed to ensure the accuracy of subsequent calculations. Next, surface normals were computed for each point to generate normal vector information. These normals played a critical role in feature matching, as they provide local geometric information that enables the Fast Point Feature Histogram (FPFH) descriptor to more accurately represent point cloud features.

FPFH was a local feature descriptor that generated a 33-dimensional feature vector by analyzing the geometric relationships between each point and its neighbors. These feature vectors were used for establishing correspondences between point clouds. To improve the robustness of the matching process, the KdTree algorithm was used to match the FPFH features between the two point clouds, thereby establishing an initial spatial mapping relationship.

Subsequently, the Sample Consensus Initial Alignment (SAC-IA) algorithm was employed to perform coarse registration. SAC-IA iteratively searched for the optimal rigid transformation matrix that aligned the source point cloud to the target point cloud, yielding an initial alignment result.

(2) Accurate registration

For the coarsely aligned point clouds, accurate registration was performed using the Iterative Closest Point (ICP) algorithm. ICP parameters were set, including maximum correspondence distance, maximum number of iterations, transformation convergence threshold, and mean square error threshold. The ICP algorithm iteratively refines the alignment by minimizing the distance between corresponding points in the source and target clouds.

In each iteration, the transformation between corresponding points was calculated, and the position of the source cloud was updated. The rotation and translation matrices were computed using the Singular Value Decomposition (SVD) method. The iteration terminated when both the changes in the rotation and translation matrices fell below their respective thresholds, or when the change in mean square error was less than a predefined value.

The final output included the precise transformation matrix and the registration error, resulting in an accurately aligned point cloud.

Calculation method of phenotypic traits for tomato plant

(1) Calculation method of plant height

Plant height was one of the most fundamental indicators in plant morphological studies and was defined as the distance from the base of the plant to the apical point of the main stem. As shown in Fig. 7, tomato plant height was calculated by determining the difference between the maximum and minimum values along the Z-axis from the 3D point cloud of the plant.

(2) Calculation method of canopy width

The canopy width of a tomato plant referred to the maximum horizontal distance across the plant at its widest point, as showed in Figure 8. The calculation of tomato canopy width involved two steps as follows:

Step 1: The point cloud was projected onto the XOY plane by ignoring the z-axis coordinates and retained only the x and y coordinates.

Step 2: On the XOY plane, the distances between all pairs of points were calculated, and the maximum value was selected. The calculation formula was as follows:

$$W = max\left(\sqrt{(x_2 - x_1)^2 - (y_2 - y_1)^2}\right) \quad (2)$$

where:

W represented the canopy width;

(x_1, y_1) and (x_2, y_2) were the coordinates of the two most distant points on the XOY plane;

A schematic diagram was shown in Fig. 8.

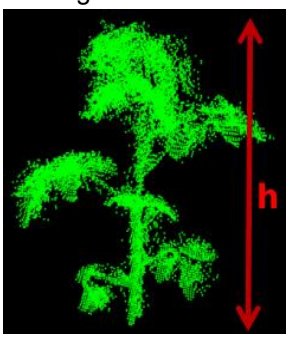

Fig. 7 - Schematic diagram of plant height calculation

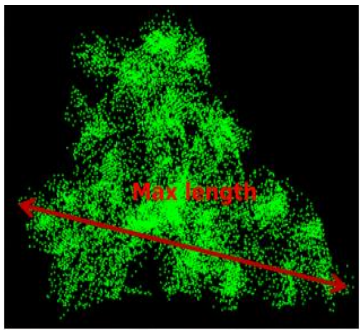

Fig. 8 - Schematic diagram for calculating canopy width

(3) Calculation method of leaf angle

The leaf angle was a crucial parameter in tomato plant physiology. Due to the complex canopy and leaf structure and significant occlusion, traditional 2D imaging methods often struggled to accurately acquire petiole angles. In this study, a method was proposed by selecting appropriate observation perspectives based on 3D point cloud modeling.

First, the optimal viewing angle was determined using the reconstructed 3D point cloud of the tomato plant to obtain the leaf angle. Then, in the reconstructed 3D space, a point A was selected on the main stem, a point C was selected on the petiole, and point B was selected at the junction of the stem and petiole. The leaf inclination angle $\angle BAC$ was calculated using the following formula:

$$cos(\angle BAC) = \frac{AB \cdot AC}{|AB| \cdot |AC|} \quad (3)$$

where, vectors *AB* and *AC* were computed as follows:

$$AB = \left(x_b - x_a,\ y_b - y_a, z_b - z_a\right) \quad (4)$$

$$AC = \left(x_c - x_a,\ y_c - y_a, z_c - z_a\right) \quad (5)$$

where:

(x_a, y_a, z_a), (x_b, y_b, z_b) and (x_c, y_c, z_c) represented the coordinates of the three points A, B, and C mentioned above, respectively;

By calculating the angle between vectors AB and AC, the leaf angle ∠BAC was obtained. A schematic diagram was shown below:

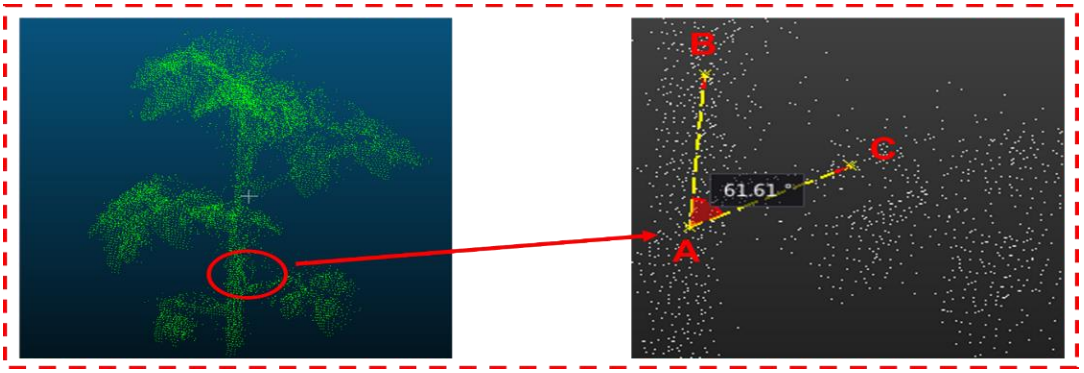

Fig. 9 - Schematic diagram for calculating leaf angle

RESULTS AND ANALYSIS

Analysis of preprocessing results

As shown in Figure 10, a comparison of the raw point clouds of tomato plants from three different viewpoints with the point clouds processed by the conditional filtering method clearly demonstrates that irrelevant background information, such as the planting pots and surrounding environment, was successfully removed. This indicates that the conditional filter can effectively extract the region of interest in 3D space. However, this method still faces challenges in dealing with near-boundary and internal noise points.

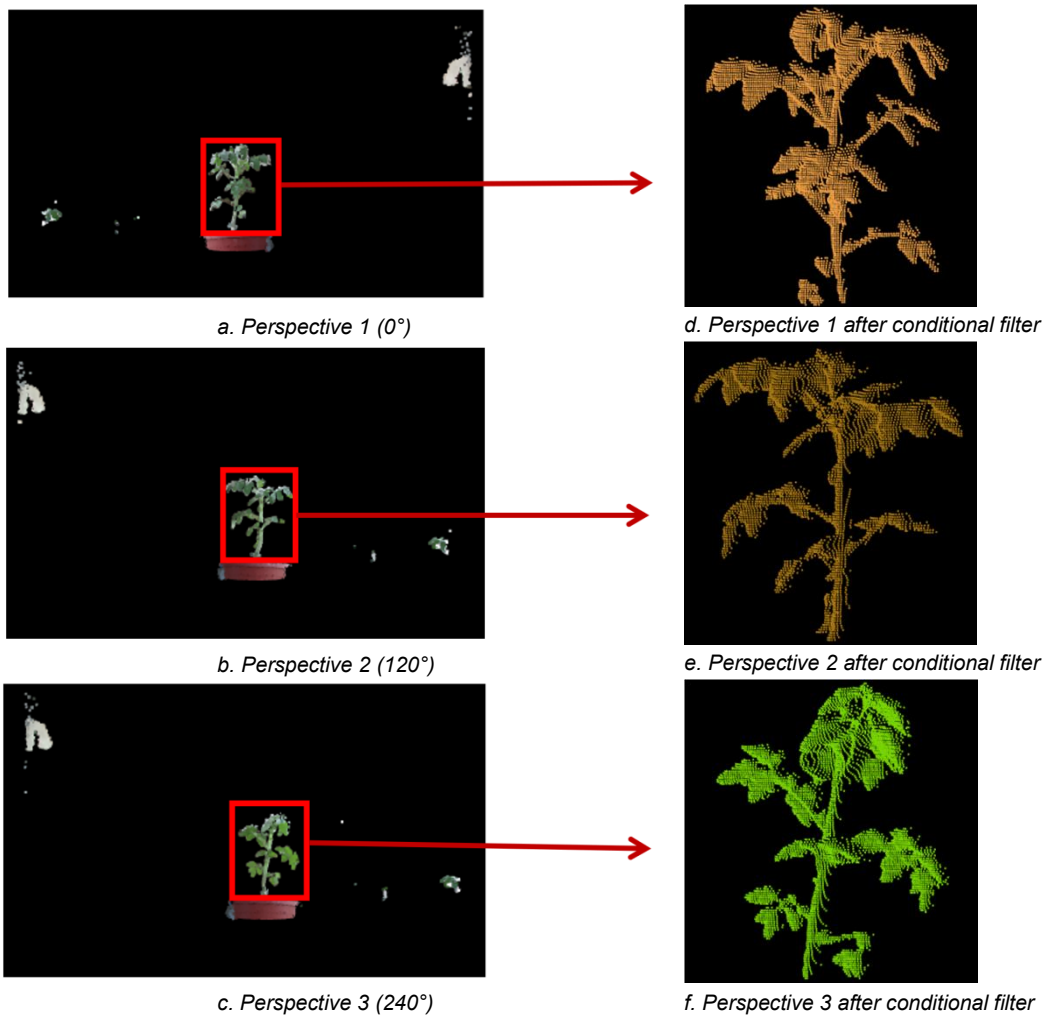

Fig. 10 - Comparison before and after conditional filter processing

To further enhance the quality of the point cloud data, Statistical Outlier Removal (SOR) filtering was introduced for additional processing. After applying the conditional filter, the number of point cloud data points in the three views was 3,818; 3,185; and 4,318, respectively. Following the application of the SOR filter, the point counts were reduced to 3,230; 2,678; and 3,600, representing reductions of 15.41%, 15.93%, and 16.70%, respectively.

This two-stage filtering approach significantly improves the efficiency of subsequent computations and enhances the accuracy of point cloud registration.

Analysis of registration results

As shown in Figure 11, the SOR-filtered tomato plant point clouds from three different viewpoints were rotated for visualization. Due to viewpoint limitations and occlusions between stems and leaves-particularly the mutual occlusion between stem and leaf structures-some data loss was inevitable, as indicated by the red arrows in the figure. This makes it difficult to comprehensively capture the complex morphology of the plant from a single view.

However, multi-view registration techniques can effectively address this limitation by aligning and fusing point cloud data obtained from different perspectives. The registered point cloud integrates information from multiple views, resulting in a more complete and accurate 3D reconstruction.

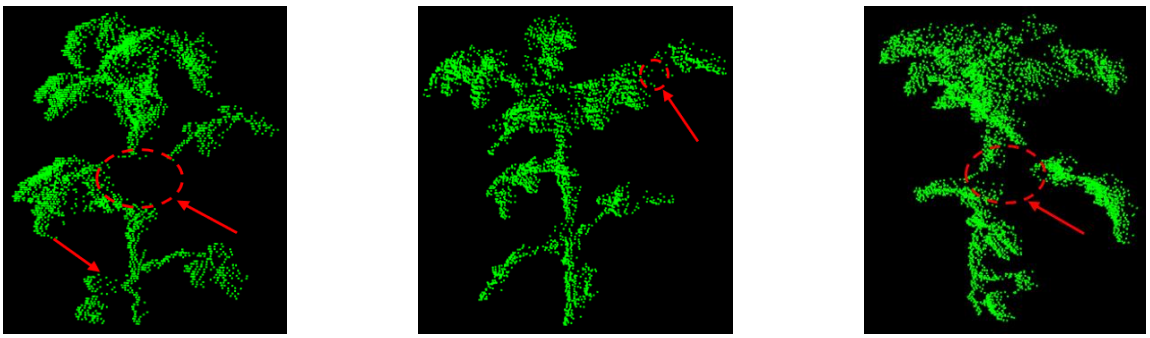

a. Perspective 1 (0°) after SOR filtering b. Perspective 2 (120°) after SOR filtering c. Perspective 3 (240°) after SOR filtering

Fig. 11 - Left view from three perspectives

As illustrated in Figure 12, the reconstructed tomato plant point cloud was rotated 45° to the left and right, respectively. These views offer a clearer observation of the reconstructed results. The rotated point clouds reveal a well-separated stem-leaf structure and a complete overall morphology. The structural details of both the stem and the leaves were distinctly visible, and the overall plant shape was accurately preserved. These results demonstrate that the registered and reconstructed 3D point cloud not only effectively compensates for data loss but also significantly improves detail capture and structural integrity in the final model.

a. left-rotated view after reconstruction b. front view after reconstruction c. right-rotated view after reconstruction

Fig. 12 - Views from different perspectives after registration and reconstruction

To further verify the accuracy of the reconstructed model, the plant height and canopy width from three single-view point clouds, each processed using conditional filtering, were calculated and compared with manually measured values. The calculation errors were shown in Fig. 13.

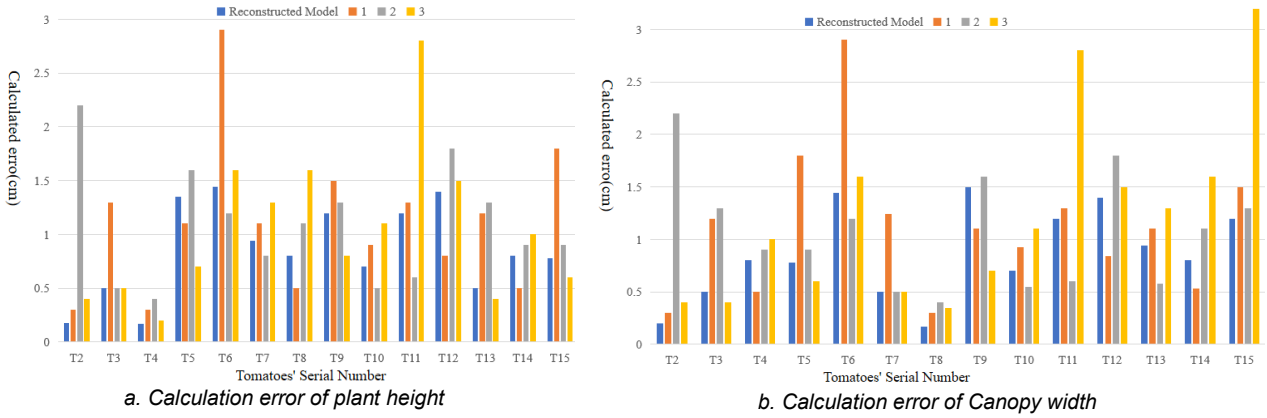

a. Calculation error of plant height b. Calculation error of Canopy width

Fig. 13 - Calculation error between the reconstructed model and single-view measurements

As shown in Figure 13(a), the error range for View 1 was 0.3–2.9 cm, with an average error of 1.14 cm. For View 2, the error ranged from 0.5–2.2 cm, with an average of 1.04 cm. For View 3, the error ranged from 0.4–2.8 cm, with an average of 1.05 cm. The error range for the reconstructed model was 0.17–1.35 cm, with an average error of 0.76 cm.

In Figure 13(b), it could be observed that the canopy width errors from the single views ranged from 0.2–3.2 cm, with an average error of 1.25 cm. In comparison, the reconstructed model yielded an error range of 0.17–1.5 cm, with an average error of 0.83 cm.

These results demonstrate that the reconstruction-based measurements produce smaller and more stable errors compared to single-view calculations, thus confirming the effectiveness of the 3D reconstruction model.

Calculation and analysis of phenotypic traits

To validate the effectiveness of the proposed phenotypic parameter estimation method based on the reconstructed 3D point cloud of tomato plants, a correlation analysis was conducted between the computed values and manually measured values. According to the phenotypic calculation methods for plant height, canopy width, and leaf angle described in Section 2.4, the corresponding values were calculated from the reconstructed tomato point clouds. Meanwhile, manual measurements of height, canopy width, and leaf angle were performed on nine tomato plants, with three repeated measurements taken for each phenotype to obtain average values. To further verify the accuracy of the method, linear correlations between the computed values and measured values were established.

For plant height, the coefficient of determination (R^2) was 0.98, and the root mean square error (RMSE) was 0.75 cm, with an error range of 0.18 cm to 1.58 cm, as shown in Figure 14(a). For canopy width, the R^2 and RMSE were 0.94 and 1.10 cm, respectively, with an error range of 0.12 cm to 2.13 cm, as shown in Figure 14(b). For leaf angle, the R^2 was 0.89 and the RMSE was 4.43 °, with an error range of 1.14 ° to 13.43 °, as shown in Figure 14(c).

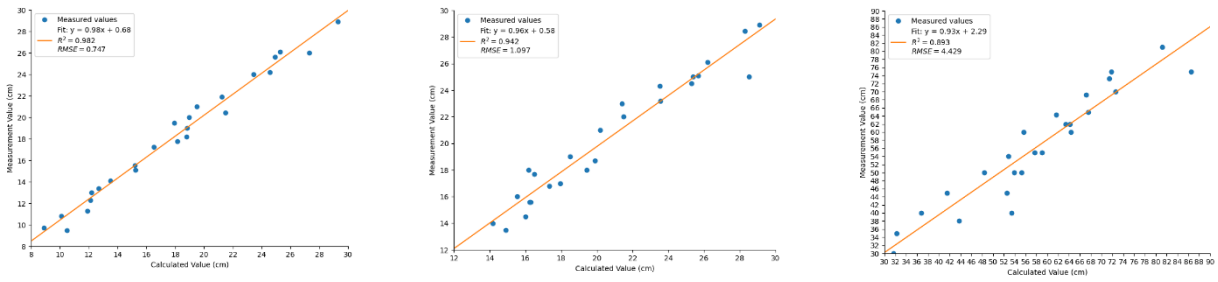

a. Height *b. Canopy Width* *c. Leaf angle*

Fig. 14 - The correlation between the calculated and measured values of phenotypic parameters

These experimental results demonstrated that the computed values for plant height, canopy width, and leaf angle from the reconstructed 3D point cloud were highly consistent with the manually measured phenotypes, confirming the validity and accuracy of the method.

The primary sources of error in estimating plant height, canopy width, and leaf angle stem from the resolution limitations of the Kinect hardware sensor. In addition, traditional manual measurements were subject to human error, which could cause slight deformation of the canopy structure and lead to inconsistencies in data acquisition before and after measurement.

CONCLUSIONS

In this study, a multi-view 3D point cloud acquisition system based on the Kinect 2.0 sensor was developed to reconstruct high-quality point cloud models of individual tomato plants. Through a preprocessing pipeline combining Conditional Filtering and Statistical Outlier Removal, along with down-sampling, background noise and redundant data were effectively eliminated, thereby enhancing computational efficiency. By applying coarse and fine registration to multi-view point clouds, the system successfully addressed issues of data loss caused by occlusion and viewpoint limitations, yielding clear and structurally complete 3D plant models. Phenotypic trait extraction from the reconstructed models demonstrated high accuracy, with average errors of 0.81 cm for plant height, 1.03 cm for canopy width, and 4.28° for leaf angle. These results validate the reliability and practicality of the proposed method, supporting its application in 3D plant modeling and lightweight phenotyping workflows. However, the current system is mainly applicable to individual plants and is limited to the extraction of several structural phenotypic traits. In future work, the proposed method will be extended to more complex planting scenarios and diverse crop populations. In addition, robust stem–leaf segmentation algorithms will be developed, and additional phenotypic parameters will be extracted to further enhance the system's applicability in comprehensive plant phenotyping studies.

ACKNOWLEDGEMENTS

This work was supported by the National Key Research and Development Program of China (Grant No. 2022YFD1900801).

REFERENCES

[1] Choi, H. B., Park, J. K., Park, S. H., & Lee, T. S. (2024). NeRF-based 3D reconstruction pipeline for acquisition and analysis of tomato crop morphology[J]. *Frontiers in Plant Science*,15, 1439086, Switzerland. DOI: 10.3389/fpls.2024.1439086

[2] Du, X., Meng, Z., Ma, Z., Lu, W., & Cheng, H. (2023). Tomato 3D pose detection algorithm based on keypoint detection and point cloud processing[J]. *Computers and Electronics in Agriculture*, 212: 108056, Netherlands. DOI: 10.1016/j.compag.2023.108056

[3] Galba, A., Masner, J., Kholová, J., Kartal, S., Stočes, M., Mikeš, V., Šimek, P., Prokopová, Š., Fiala, R., Karrer, T., & Tóth, A. (2025). Annotated 3D Point Cloud Dataset of Broad-Leaf Legumes Captured by High-Throughput Phenotyping Platform. *Scientific Data*, 12(1), 1764, United Kingdom. DOI: 10.1038/s41597-025-06049-7

[4] Geng Y.L., Yue X.D., Ji Y.K., Li Y.B., Fu Y.F., & Ya S.C. (2023). Research on pig body size measurement system based on stereo vision[J]. *INMATEH-Agricultural Engineering*, 70(2), pp.76-85. Bucharest/Romania. DOI: 10.35633/inmateh-70-07

[5] Hadadi, M., Saraeian, M., Godbersen, J., Jubery, T. Z., Li, Y., Attigala, L., Balu, A., Sarkar, S., Schnable, P.S., Krishnamurthy, A., & Ganapathysubramanian, B. (2025). Procedural generation of 3D maize plant architecture from LiDAR data[J]. *Computers and Electronics in Agriculture*, 236, 110382, Netherlands. DOI:10.1016/j.compag.2025.110382

[6] James, C., Chandra, S. S., & Chapman, S. C. (2025). A scalable and efficient UAV-based pipeline and deep learning framework for phenotyping sorghum panicle morphology from point clouds[J]. *Plant Phenomics*, 7(2), 100050, United States. DOI:10.1016/j.plaphe.2025.100050

[7] Jiang, Y., Liu, Q., Lu, W., Zhou, B., Smoleňová, K., Tekinerdogan, B., & Yang, Q. (2025). Plant stem occlusion inpainting with Deep Reinforcement Learning[J]. *Computers and Electronics in Agriculture*, 237: 110465, Netherlands. DOI:10.1016/j.compag.2025.110465

[8] Jing, L., Wei, X., Song, Q., & Wang, F. (2023). Research on estimating rice canopy height and LAI based on LiDAR data[J]. *Sensors*, 23(19): 8334, Basel/Switzerland. DOI: 10.3390/s23198334

[9] Mach, J., Svatý, Z., Šoupa, O., Nouzovský, L., & Halecký, M. (2025). Implementation of an SfM-MVS-based photogrammetry approach for detailed 3D reconstruction of plants[J]. *Plant Methods*, 21(1), 127, United Kingdom. DOI: 10.1186/s13007-025-01445-x

[10] Miao, Y., Li, S., Wang, L., Li, H., Qiu, R., & Zhang, M. (2023). A single plant segmentation method of maize point cloud based on Euclidean clustering and K-means clustering[J]. *Computers and Electronics in Agriculture*, 210: 107951, Netherlands. DOI: 10.1016/j.compag.2023.107951

[11] Qi, J., Gao, F., Wang, Y., Zhang, W., Yang, S., Qi, K., & Zhang, R. (2025). Multiscale phenotyping of grain crops based on three-dimensional models: A comprehensive review of trait detection[J]. *Computers and Electronics in Agriculture*, 237: 110597, Netherlands. DOI: 10.1016/j.compag.2025.110597

[12] Rossi, R., Costafreda-Aumedes, S., Summerer, S., Moriondo, M., Leolini, L., Cellini, F., Bindi, M., & Petrozza, A. (2022). A comparison of high-throughput imaging methods for quantifying plant growth traits and estimating above-ground biomass accumulation[J]. *European Journal of Agronomy*, 141, 126634, Netherlands. DOI: 10.1016/j.eja.2022.126634

[13] Schunck, D., Magistri, F., Rosu, R.A., Cornelißen, A., Chebrolu, N., Paulus, S., Léon, J., Behnke, S., Stachniss, C., Kuhlmann, H., & Klingbeil, L. (2021). Pheno4D: A spatio-temporal dataset of maize and tomato plant point clouds for phenotyping and advanced plant analysis [J]. *Plos one*, 16(8), e0256340, USA. DOI: 10.1371/journal.pone.0256340

[14] Shi B., Guo L., & Yu L. (2025). Accurate LAI estimation of soybean plants in the field using deep learning and clustering algorithms[J]. *Frontiers in Plant Science*, 15: 1501612, Sanya/China. DOI: 10.3389/fpls.2024.1501612

[15] Sun L.L., Li Y.Y., Wang Y.Z., Shi, W.J., Zhang, W.P., Zhang, X.Y., Zhao, H.M., & Li, F.Z. (2023). Study on phenotypic characteristics of millet based on 3D MODEL[J]. *INMATEH-Agricultural Engineering*, 69(1), pp.579-588, Bucharest/Romania. DOI: 10.35633/inmateh-69-55

[16] Sun Y.Y., Wang X.C., & Zhang K.X. (2023). Three-dimensional reconstruction and character extraction of corn plants based on Kinect sensor [J]. *INMATEH-Agricultural Engineering*, 69(1), pp. 635-644. Bucharest/Romania. DOI: 10.35633/inmateh-69-61

[17] Timprae, W., Sagawa, T., Baar, S., Kondo, S., Okada, Y., Sato, K., Rumahorbo, P.S., Lyu, Y., Shibuya, K., Gama, Y., & Hatanaka, Y. (2025). Tomato Growth Monitoring and Phenological Analysis Using Deep Learning-Based Instance Segmentation and 3D Point Cloud Reconstruction[J]. *Sustainability*, 17(22), 10120, Basel/Switzerland. DOI: 10.3390/su172210120

[18] Vázquez-Arellano, M., Paraforos, D. S., Reiser, D., Garrido-Izard, M., & Griepentrog, H. W. (2018). Determination of stem position and height of reconstructed maize plants using a time-of-flight camera[J]. *Computers and Electronics in Agriculture*, 154, 276-288, Netherlands. DOI: 10.1016/j.compag.2018.09.006

[19] Zermas, D., Morellas, V., Mulla, D., & Papanikolopoulos, N. (2020). 3D model processing for high throughput phenotype extraction–the case of corn[J]. *Computers and Electronics in Agriculture*, 172, 105047, Netherlands. DOI: 10.1016/j.compag.2019.105047

[20] Zuo H.X., Huang Q.C., Yang J.H., Meng F.J., Li S.E., & Li L. (2023). In Situ Identification Method of Maize Stalk Width Based on Binocular Vision and Improved YOLOv8 (基于双目视觉和改进 YOLOv8 的玉米茎秆宽度原位识别方法)[J]. *Smart Agriculture*, 5(03):86-95, Beijing/China. DOI: 10.12133/j.smartag.SA202309004